RSC Advances

ROYAL SOCIETY OF CHEMISTRY

www.rsc.org/advances

For table of contents entry only

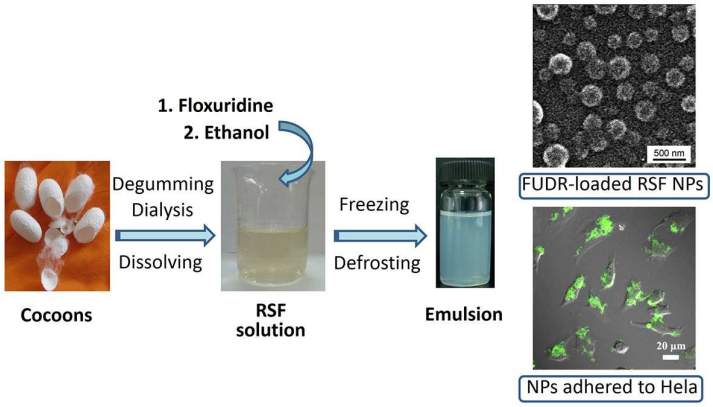

A clinical used anti-cancer drug floxuridine was successfully encapsulated in silk fibroin nanospheres. Such drug-load nanospheres have controllable size, fair drug-loading capacity and controlled release property, which maybe a good candidate for lymphatic chemotherapy.

Cite this: DOI: 10.1039/c0xx00000x

www.rsc.org/xxxxxx

PAPER

Floxuridine-loaded silk fibroin nanospheres

Shuying Yu[a], Wenhua Yang[a], Sheng Chen[b], Mengjie Chen[a], Yezhuo Liu[c], Zhengzhong Shao[a] and Xin Chen*[a]

Received (in XXX, XXX) Xth XXXXXXXXX 20XX, Accepted Xth XXXXXXXXX 20XX

DOI: 10.1039/b000000x

Silk protein is a very promising biomedical material due to its renewability, nontoxicity, biocompatibility, and biodegradability. In this communication, we report our attempt to use regenerated silk fibroin (RSF) as a drug-carrier to encapsulate hydrophilic anti-cancer drug floxuridine (FUDR). The FUDR-loaded RSF nanospheres with the average sizes ranging from 210 to 510 nm are prepared by using a facile and clean method developed in this laboratory previously based on the self-assembly of silk protein. The maximum drug loading is about 6.8% and the release time of such a kind of FUDR-loaded RSF nanospheres is more than 2 days. The FUDR-loaded RSF nanospheres are found to be able to adhere onto the Hela cells easily. The FUDR loaded in the RSF nanospheres exhibits the similar curative effect to kill or inhibit Hela cells to the free FUDR. All these results imply that such a kind of biomacromolecule based anti-cancer drug nanocarrier has a great potential for the lymphatic chemotherapy in clinical applications.

Introduction

Biomacromolecules like cellulose, albumin and chitosan that own unique properties of biocompatibility, biodegradability, non-toxicity and renewability[1-3] have attracted more and more attention as drug delivery systems in the past few decades.[4,5] Compared to conventional dosage forms, nanoparticles have the ability to deliver many kinds of drugs to targeted areas of the body and release them for a period of time,[6] showing numerous advantages, including improved drug therapeutic effect, patient compliance and convenience, and reduced toxicity.[7,8]

Regenerated silk fibroin (RSF) from *Bombyx mori* silk is one of the fibrous proteins (does not have bioactivity, so often be used as a biomaterial) that has been widely used in biomedical and pharmaceutical fields.[9-11] It consists of large hydrophobic regions, segregated by the relatively short and more hydrophilic regions.[12] RSF is water soluble by adopting random coil and/or helical conformation, but easily becomes water insoluble when takes a conformation transition to β-sheet induced by various factors, such as organic solvents,[13] shear force,[14] sonication,[15] the increase of temperature,[16] and the change of pH value.[17] That implies RSF has the characteristics of self-assembly, providing the unique opportunity in design of supramolecular structures. In addition, silk fibroin exhibits good biocompatibility,[18] controllable biodegradability[19] and low inflammatory responses,[20] further suggesting it is an ideal candidate for nanoscale drug-delivery carrier.

Several efforts have been made to develop RSF nanospheres. For example, RSF nanospheres with the size of 300–400 nm were prepared by dissolving polyvinyl alcohol part in silk fibroin/polyvinyl alcohol blend and were utilized to load model drugs tetramethylrhodamine conjugated bovine serum albumin (TMR-BSA), tetramethylrhodamine conjugated dextran (TMR-Dextran), and rhodamine B (RhB).[21] In another study, RSF nanospheres with the size of 150–170 nm, preparing by desolvation technique demonstrated the sustained *in vitro* release of entrapped vascular endothelial growth factor (VEGF) over 3 weeks and the efficient intracellular uptake by murine squamous and carcinoma cells.[22] It was also reported that RSF nanospheres can be prepared by simply dropwise adding RSF solution into the water-miscible protonic and polar aprotonic organic solvents.[23] In our previous work, we invented a facile and clean method to prepare RSF nanospheres with predictable and controllable particle sizes based on the self-assembly of silk protein.[24,25] The particle size of our RSF nanospheres covered a wide range, e.g., from 200 to 1000 nm. Later on, we successfully prepared RSF nanospheres carrying hydrophobic anti-cancer drug paclitaxel by using the similar technique.[26] The drug loading of such RSF nanospheres was about 6.9% and the release time was over 9 days.

In this communication, we show our attempt to use RSF nanospheres as a carrier for a hydrophilic anti-cancer drug floxuridine (FUDR). FUDR is a widely used primary clinical anti-cancer drug in the treatment of colon carcinoma and colorectal cancer.[27] However, its adverse effects associated with chemotherapeutics as many other anticarcinogen are still unresolved.[28] Although some efforts have been made to minimize the side effects and maximize the therapeutic efficacy of FUDR, they were mostly focused on the synthesis of its prodrugs that always involved relatively complicated chemical reactions.[29-31] Only few reports were about the use of biomaterials such as human albumin[32] and liposomes[33] to be the drug carrier to decrease the side effects of FUDR. Therefore, based on the our previous work,[24-26,34-36] we selected silk protein as a biomacromolecular carrier to synthesize FUDR-loaded RSF

nanospheres in order to increase the drug release time and reduce the severe side effect of pristine FUDR.

Our designed purpose for the FUDR-loaded RSF nanospheres is to apply them to lymphatic chemotherapy. Lymphatic chemotherapy is a relatively new therapeutic modality and has been applied for the treatment of lymphatic metastases in patients with digestive tract and lung cancers.[37,38] Not like the conventional intravenous chemotherapy, the main approaches to achieve lymphatic chemotherapy consist of the use of drug delivery system and local interstitial administration such as intramuscular, subcutaneous, intratumoral and intraperitoneal injection for the targeting of agents to regional lymph nodes. Particles have been observed passing through the lymphatic vessels but not the blood capillaries mainly due to the difference in permeability, which may enhance chemo-responsiveness while reducing adverse systemic effects.[38] The studies on drug-loaded liposomes and PLGA particles show that the particle size from several hundred nanometer to several micrometer is good for lymphatic chemotherapy because the smaller particles pass unretarded through the lymph nodes but the larger ones are easy to be predominantly entrapped by lymph node tissues during physical filtration, and thus achieve long time drug release.[39-42]

Experimental

Materials

The cocoons of *B. mori* silkworm were obtained from Jiangsu Province, China. FUDR was purchased from Hubei Prosperity Galaxy Chemical Co., Ltd. (China). Ethanol was purchased from Shanghai Zhenxin Chemicals Factory (China). Fluorescein isothiocyanate (FITC) and methoxypolyethylene glycol amine (mPEG-NH_2) were purchased from Aladdin. DMSO, DMEM (Dulbecco's modified Eagle's medium) were obtained from Acros. The Hela line was provided by the Institute of Biochemistry and Cell Biology, SIBS, Chinese Academy of Science. All other chemicals were analytical grade and used without further purification.

Preparation of RSF aqueous solution

The *B. mori* silkworm cocoons were cut into small pieces and boiled for 60 min in 0.02 mol/L Na_2CO_3 aqueous solution, and then washed with de-ionized water for several times. After drying completely, the degummed silk was dissolved in 9.5 mol/L LiBr at 45 °C for 1 h. The solution was then dialyzed in a semipermeable cellulose tube (12-14 kDa MWCO) against de-ionized water for 3 days to remove the salt. Afterward, the dialyzed silk fibroin solution was centrifuged at 8000 r/min for 10 min and the supernatant was collected, and then stored at 4 °C for further use. The final concentration of RSF solution was about 40 mg/mL by weight method.

Preparation of FUDR-loaded RSF nanospheres

Certain amount of FUDR aqueous solution (10 mg/mL) was added into RSF solution under gently stirring. The final RSF concentration was set to 10, 20, and 40 mg/mL, and the mass ratio of FUDR to RSF was set to 0.125, 0.25, and 0.375, respectively. After stirring for 20 min, the absolute ethanol with the volume ratio of $V_{RSF}/V_{ethanol}$ = 5/2 was slowly added by dropwise. Afterward, the mixture was gently stirred for 3 min and incubated in a refrigerator at -20 °C for 20 h. After defrosting at room temperature, a milky emulsion was found. Finally, mPEG-NH_2 aqueous solution (mass ratio of mPEG-NH_2 to nanospheres was set to 1) was added slowly under gently stirring, and continued to stir for 5 h. To remove the non-encapsulated drug, the suspensions were ultracentrifuged at 20,000 r/min for 3 min and the resulted FUDR-loaded RSF nanospheres were re-suspended with de-ionized water.

Preparation of FITC-labeled FUDR-loaded RSF nanospheres

FITC is used for labelling RSF nanospheres to monitor their cellular uptake property. Synthesis of FITC labelled RSF nanospheres was based on the reaction between the isothiocyanate groups in FITC and the primary amino groups in RSF.[43] Briefly, 5 mg FITC (dissolved in 5 mL DMSO) was added to 10 mL FUDR-loaded RSF nanospheres suspension. The reaction was allowed to proceed for 12 h in the dark at room temperature.

Characterizations

Size and zeta potential analysis. Size and zeta potential of FUDR-loaded RSF nanospheres were analyzed at 37±0.1 °C with Zetasizer Nano from Malvern.

Morphology observations. The as-prepared emulsion was diluted with de-ionized water before SEM and TEM observation. SEM images of RSF nanospheres were obtained with Hitachi S-4800 high-resolution SEM at 20 kV. TEM images were obtained with Tecnai G2 at 200 kV.

Encapsulation and *in vitro* release of FUDR. The amount of free FUDR in the supernatant after ultracentrifugation was determined with Hitachi UV 2910 UV-vis spectrometer. The drug loading capacity was calculated as follows.

$$Drug\ loading = \frac{Amount\ of\ FUDR\ in\ RSF\ nanospheres}{Amount\ of\ total\ FUDR-loaded\ RSF\ nanospheres} \times 100\%$$

To study the *in vitro* release of FUDR from the drug-loaded RSF nanospheres, the ultracentrifuged nanospheres were re-suspended with de-ionized water to a certain concentration. Then, 1 mL such emulsion was put into the dialysis tube, immersing in 10 mL PBS buffer solution (pH=7.4, 37±0.1 °C). At a certain time point, the FUDR concentration in PBS was determined by UV-vis spectrometer and the dialysis tube was transferred into another 10 mL fresh PBS solution.

***In vitro* cytotoxicity assay with MTT.** Hela cells were grown in culture media DMEM and seeded in 96-well plates at a density of 10,000 cells/well at 37 °C under 5% CO_2. After 12 h, the culture media were removed and replaced with fresh medium containing different amount of pristine RSF nanospheres. After 24 h, 20 μL of MTT dye solution (Sigma-Aldrich) was added to each well and incubated for an additional 4 h. Then the medium was removed and the formazan crystals were dissolved with 200 μL of DMSO. An enzyme-linked immunosorbent assay (ELISA) reader (Infinite M200, Tecan, Astraia) was then used to measure the luminescence intensity at 490 nm of each well. The relative cell

viability (%) related to the control sample that incubated with cell culture medium without RSF nanospheres was calculated by follows:

$$\text{Cell viability (\%)} = [A]_{test} / [A]_{control} \times 100\%$$

where $[A]_{test}$ is the absorbance of the test sample and $[A]_{control}$ is the absorbance of the control sample.

***In vitro* cellular uptake of FUDR-loaded RSF nanospheres.** To check the interaction between cells and drug-loaded RSF nanospheres, the Hela cells were incubated with FITC-labeled FUDR-loaded RSF nanospheres for 2 h and then washed with de-ionized water three times. Afterward, the cells were observed with an Olympus FlouView FV1000 confocal fluorescence microscope (λ_{em}=490 nm, λ_{ex}=520 nm).

The anti-proliferative activity of free FUDR and FUDR-loaded RSF nanospheres. The anti-proliferative activity of FUDR-loaded RSF nanospheres was evaluated by the MTT assay using the Hela cell line. The procedure is similar to the *in vitro* cytotoxicity assay described above but replaced pristine RSF nanospheres by FUDR-loaded RSF nanospheres. The incubation time with the FUDR-loaded RSF nanospheres was set as 3 h and 24 h. As a control group, Hela cells were also incubated with the pure FUDR solutions, in which the amount of FUDR was set as the same as in the corresponding drug-loaded RSF nanospheres.

Results and discussion

Formation and characterization of FUDR-loaded RSF nanospheres

Similar to the paclitaxel-loaded RSF nanospheres we reported previously,[26] FUDR-loaded RSF nanospheres with controllable size were obtained based on the self-assembly of silk fibroin by adding ethanol into the FUDR–RSF mixture solution and then subjecting to freeze. Although the as-prepared FUDR-loaded RSF nanospheres emulsion was very stable, which can be stored at room temperature for at least 1 month without apparent aggregation, we found the nanospheres seemed not easy to well re-disperse in buffer solution after they were centrifuged from the emulsion. In order to increase the re-dispersed capability and the stability of FUDR-loaded RSF nanospheres in the buffer solution, we introduced mPEG-NH_2 to the surface of nanospheres. We suppose the interaction between RSF and PEG is mainly the electrostatic force between the negative charges on RSF nanospheres and the positive charges on ammonium on mPEG-NH_2 as the zeta potential of RSF nanospheres ([RSF] = 40 mg/mL, FUDR/RSF = 0.375] increases from −34.3±3.4 mV to −22.1±2.8 mV after PEGylation, according with the changes observed in other works,[44,45] proving mPEG-NH_2 was successfully attached. After modification, the PDI of RSF nanospheres in the re-dispersed solution was found to drop from 0.452 to 0.082. The main reason for the improvement on the uniformity of the re-dispersed nanospheres after such a PEGylation was thought to be the steric repulsion effects of the tethered PEG strands attached on the surface of nanospheres as reported in the literature.[46,47]

It is expected that after loading drugs, the size of the RSF nanospheres increased. In this case, it changed from 260 nm to 510 nm when the mass ratio of FUDR to RSF (FUDR/RSF) was 0.375 (Table 1). In the meantime, by varying the initial RSF concentration in the reaction system ([RSF]) as well as FUDR/RSF, we can obtain FUDR-loaded RSF nanospheres with different sizes. The increase in RSF concentration also made the nanospheres lager, for example, from 210 nm to 480 nm when the concentration was from 10 to 40 mg/mL. That is to say we are able to synthesize the FUDR-loaded RSF nanospheres with the particle size from 200 to 500 nm, which is suitable for lymphatic chemotherapy.[39-42]

Both SEM and TEM images demonstrate that the FUDR-loaded RSF nanospheres are spherical granules without apparent aggregation (Fig. 1, S1). In addition, it can be seen more directly that the size of the nanospheres changed with the preparation conditions. For instance, the particle size of nanospheres shown in Fig. 1 is 185±33 nm (n=32) and 277±27 nm (n=27), which accords with the difference shown in their hydrodynamic diameters (290 nm and 510 nm, Table 1). Of course, the particle sizes shown in SEM and TEM are relatively smaller than the ones measured by dynamic light scattering, as the nanospheres were in dry state in SEM and TEM but in swollen state in the latter. In addition, the comparison of the particle sizes in TEM images for the pristine and drug-loaded RSF nanospheres with the same RSF concentration further supports the conclusion for the successful drug encapsulation. The particle sizes in Fig. S1d ([RSF] = 40 mg/mL) and S1e ([RSF] = 20 mg/mL) were obviously larger than those in Fig. S1a and S2.

Table 1 Hydrodynamic diameters of FUDR-loaded RSF nanospheres prepared with different [RSF] and FUDR/RSF mass ratio.

Sample	[RSF] (mg/mL)	FUDR/ RSF	Size (nm)	PDI
1	40	0	260	0.099
2	40	0.125	400	0.107
3	40	0.25	480	0.188
4	40	0.375	510	0.060
5	20	0.25	290	0.156
6	10	0.25	210	0.081

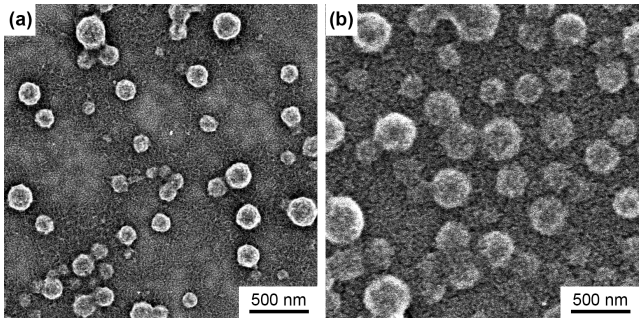

Fig. 1 SEM images of FUDR-loaded RSF nanospheres. (a) [RSF] = 20 mg/mL, FUDR/RSF = 0.25; (b) [RSF] = 40 mg/mL, FUDR/RSF = 0.375.

Drug loading and *in vitro* drug release of FUDR-loaded RSF nanospheres

The drug loading capacity of FUDR-loaded RSF nanospheres increased with increase in the initial RSF concentration as shown in Fig. 2. This may due to the weak self-assembly ability of RSF

at low concentration, which led the small encapsulation of the drug. In the meantime, the drug loading capacity also became larger when FUDR/RSF ratio was increased, but the extent of the improvement was not significant. We found the highest drug loading reached 6.8% when [RSF] = 40 mg/mL and FUDR/RSF = 0.375. However, we are unable to increase the initial RSF concentration further, as the RSF solution tends to be gelation rather than to form nanospheres.

In vitro drug-release curves of FUDR-loaded RSF nanospheres are shown in Fig. 3. Three samples with different size and drug loading capacity were compared. All samples showed a burst phase of release for about 5 h, which was probably from those drugs adsorbed on the surface and/or in the outer layer of the nanospheres. For the sample prepared from the low RSF concentration ([RSF] = 10 mg/mL), which has the smallest particle size (Table 1) and the lowest drug loading capacity (Fig. 2), it exhibited the fastest release rate (Fig. 3, curve a), reaching the equilibrium at about 30 h. On the other hand, those FUDR-loaded RSF nanospheres made from high RSF concentration ([RSF] = 40 mg/mL) showed much better controlled release behavior (Fig. 3, curve c). The portion of the burst release phase was small and the drug-release time was more than 2 days. In addition, we compared the drug-release behavior of the drug-loaded nanospheres with the same RSF concentration but different FUDR loading capacity (Fig. S3). It shows that the drug-release curve does not have much difference for the same RSF concentration, but more drug was released from those nanospheres with relatively high drug-loading capacity. However, compared to insoluble drug-carrier system, *i.e.*, paclitaxel-loaded RSF nanospheres we reported previously,[26] the release time is shorter. We assume the reason is that the hydrophilic FUDR drug was entrapped in the hydrophilic amorphous region of the RSF nanospheres, not like the hydrophobic drug was in the hydrophobic crystalline region.[48] Therefore, the drug obviously released much easier from the hydrophilic amorphous region than the hydrophobic crystalline region in the buffer solution.

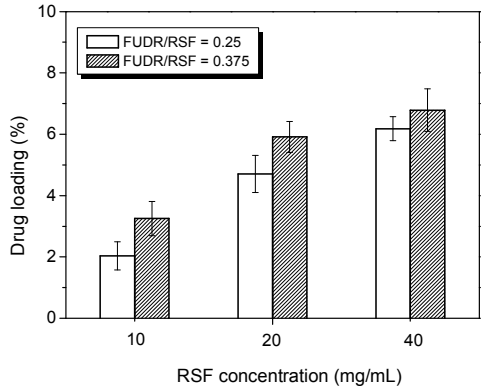

Fig. 2 Drug loading capacity of FUDR-loaded RSF nanospheres prepared with different initial RSF concentration and FUDR/RSF mass ratio.

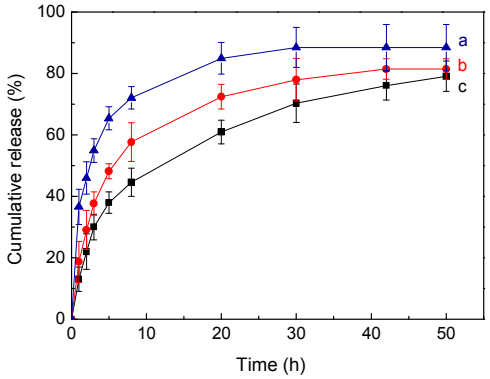

Fig. 3 *In vitro* drug-release curves of FUDR-loaded RSF nanospheres prepared when FUDR/RSF = 0.375. (a) [RSF] = 10 mg/mL, FUDR loading = 3.3%; (b) [RSF] = 20 mg/mL, FUDR loading = 6.3%; (c) [RSF] = 40 mg/mL, FUDR loading = 6.8%.

In vitro cytotoxicity of RSF nanospheres

The cytotoxicity of pristine RSF nanospheres were evaluated with Hela cells by MTT assay, and the results are shown in Fig. 4. It indicates that cells incubated with RSF nanospheres with low concentration (100 μg/mL) remained almost the same viability as the control. The cell viability decreased slowly with the increase in the concentration of RSF nanospheres, but was still about 80% when the concentration of RSF nanospheres was as high as 1.2 mg/mL. That is to say the cytotoxicity of RSF nanospheres themselves is quite small.

In vitro cellular uptake of FUDR-loaded RSF nanospheres

Before we started to study the cellular uptake of RSF nanospheres, we observed their stability in culture media DMEM. After we

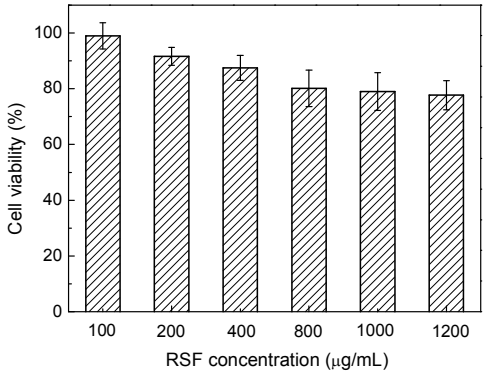

Fig. 4 Cytotoxicity of pristine RSF nanospheres with Hela cells after 24 h incubation.

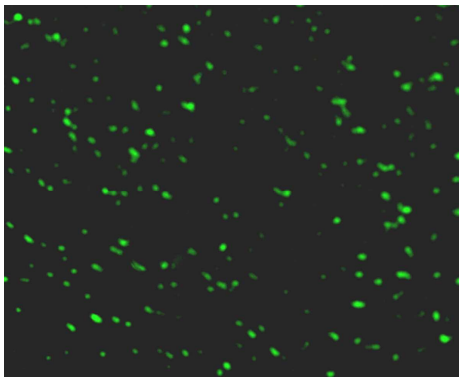

Fig. 5 Fluorescence microscopic image of FITC labeled RSF nanospheres in DMEM.

dispersed FITC labelled RSF nanospheres in DMEM for 24 h, it shows that the nanospheres remain stable and without obvious aggregation with fluorescence microscopy (Olympus BX-51, Japan) (Fig. 5). Afterward, we incubated Hela cells with the FUDR-loaded RSF nanospheres for 2 h. After thoroughly rinsing with de-ionized water, the cells were observed by confocal microscope. The images shown in Fig. 6 clearly show that the nanospheres are readily adhered to the cells. This gives a good basis for the drug-loaded RSF nanospheres to kill or inhibit cancer cells.

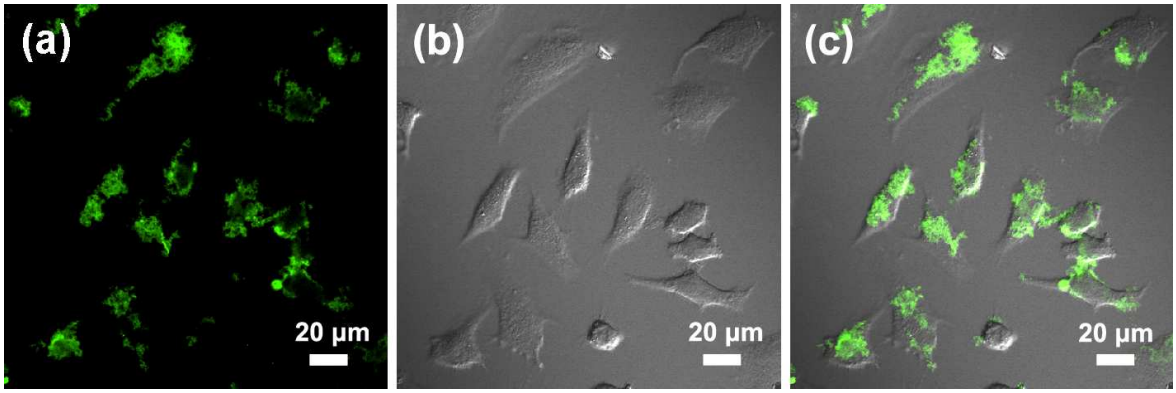

Fig. 6 Confocal microscopic images of FUDR-loaded RSF nanoparticles after incubating with Hela cells for 2 h. (a) luminescence; (b) brightfield; (c) overlay.

In vitro cellular growth inhibition of Hela cells with FUDR-loaded RSF nanospheres

Fig. 7 shows the viability of Hela cells after contacting with FUDR-loaded RSF nanospheres for 3 h and 24 h, respectively. It was expectable that with the increase in the amount of FUDR-loaded RSF nanospheres in the culture medium and the contact time, more Hela cells were killed or inhibited because more FUDR drugs were released. When the FUDR concentration in the culture medium was 100 μg/mL, less than 20% Hela cells were alive after 24 h of incubation. To evaluate the anti-cancer efficiency of the drug after encapsulating in the RSF nanospheres, we used free FUDR drug to compare. Generally, free FUDR killed or inhibited more Hela cells compared to the FUDR-loaded RSF nanospheres under the same FUDR concentration. It is understandable because first, the FUDR entrapped in the RSF nanospheres needs time to release, and second, not all FUDR released at 24 h that can be found from the release curves shown in Fig. 3. What we need emphasis is there is no large difference between the use of free FUDR and FUDR-loaded RSF nanospheres. However, in the real clinical treatment, free FUDR given by traditional intravenous administration cannot stay in lesion location for long time because of blood circulation. In lymphatic chemotherapy, the injected free FUDR may also transport to the whole body by blood and lymph circulation, but for large FUDR-loaded RSF nanospheres, they are expected to be trapped in lymph nodes and have relatively long time to release the drug towards cancer tissues. Therefore, the advantage of such FUDR-loaded RSF nanospheres is obvious.

Conclusions

In this article, we report the synthesis of a natural polymer based nanocarrier to encapsulate a hydrophilic anti-cancer drug. That is FUDR-loaded RSF nanospheres were successfully prepared by an easy and mild method, in which only the addition of ethanol and freezing RSF-ethanol solution were involved. The characterizations from dynamic light scattering and SEM/TEM observation show that FUDR-loaded RSF nanospheres have a controllable shape and size, without apparent aggregation. The size of such FUDR-loaded RSF nanospheres is from 200 to 500 nm that maybe a good candidate for lymphatic chemotherapy. In addition, the FUDR-loaded RSF nanospheres are found to be easily adhered onto the Hela cells, which is advantageous for the

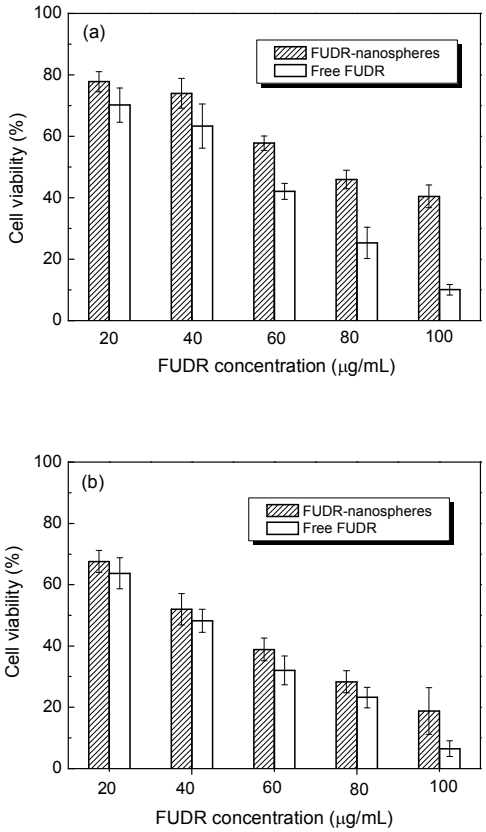

Fig. 7 Viability of Hela cells after contacting free FUDR and FUDR-loaded RSF nanospheres solutions for 3 h (a) and 24 h (b).

kill or inhibition of cancer cells. In some optimal conditions, the *in vitro* release time of FUDR-loaded RSF nanospheres is more than 2 days. After 24 h of incubation, FUDR-loaded RSF nanospheres kill or inhibit more than 80% Hela cells, implying such an anti-cancer drug nanocarrier has a great potential in future clinical treatments.

Acknowledgements

This work was supported by the Specialized Research Fund for the Doctoral Program of Higher Education, MOE of China (No. 20110071110008) and the National High Technology Research and Development Program of China (863 Program) (No. 2012AA030309). We thank Dr. Jinrong Yao and Dr. Yuhong Yang for their valuable suggestions and discussions.

Notes and references

[a] *State Key Laboratory of Molecular Engineering of Polymers, Department of Macromolecular Science, Laboratory of Advanced Materials, Fudan University, Shanghai, 200433, China.. Fax: 86 21 5163 0300; Tel: 86 21 6564 2866; E-mail: chenx@fudan.edu.cn*

[b] *Department of General Surgery, Ruijin Hospital, Shanghai Jiaotong University School of Medicine, Shanghai, 200025, China.*

[c] *Booocle Pharmaceutical Technology Co., Ltd., 1883 South Huicheng Road, Shanghai, 201821, China*

† Electronic Supplementary Information (ESI) available: TEM images of pristine and FUDR-loaded RSF nanospheres, the comparison of drug-release behavior of the drug-loaded nanospheres with the same RSF concentration but different FUDR loading capacity. See DOI: 10.1039/b000000x/

1. S. Hornig and T. Heinze, *Biomacromolecules*, 2008, **9**, 1487.
2. B. Elsadek and F. Kratz, *J. Control. Release*, 2012, **157**, 4.
3. T. Kean and M. Thanou, *Adv. Drug Delivery Rev.*, 2010, **62**, 3.
4. J. Kopecek, *Mol. Pharm.*, 2010, **7**, 922.
5. R. Langer, *Acc. Chem. Res.*, 1999, **33**, 94.
6. K. W. Leong and H. Sung, *Adv. Drug Delivery Rev.*, 2013, **65**, 757.
7. M. Rajam, S. Pulavendran, C. Rose and A. B. Mandal, *Int. J. Pharm.*, 2011, **410**, 145.
8. A. MaHam, Z. W. Tang, H. Wu, J. Wang and Y. H. Lin, *Small*, 2009, **5**, 1706.
9. G. H. Altman, F. Diaz, C. Jakuba, T. Calabro, R. L. Horan, J. Chen, H. Lu, J. Richmond and D. L. Kaplan, *Biomaterials*, 2003, **24**, 401.
10. C. Vepari and D. L. Kaplan, *Prog. Polym. Sci.*, 2007, **32**, 991.
11. E. Wenk, H. P. Merkle and L. Meinel, *J. Control. Release*, 2011, **150**, 128.
12. K. Mita, S. Ichimura and T. C. James, *J. Mol. Evol*., 1994, **38**, 583.
13. X. Chen, Z. Z. Shao, N. S. Marinkovic, L. M. Miller, P. Zhou and M. R. Chance, *Biophys. Chem.*, 2001, **89**, 25.
14. C. Mo, C. Holland, D. Porter, Z. Z. Shao and F. Vollrath, *Biomacromolecules*, 2009, **10**, 2724.
15. X. Wang, J. A. Kluge, G. G. Leisk and D. L. Kaplan, *Biomaterials*, 2008, **29**, 1054.
16. A. Motta, L. Fambri and C. Migliaresi, *Macromol. Chem. Phys.*, 2002, **203**, 1658.
17. X. H. Zong, P. Zhou, Z. Z. Shao, S. M Chen, X. Chen, B. W. Hu, F. Deng and W. H. Yao, *Biochemistry*, 2004, **43**, 11932.
18. A. S. Kon'kov, O. L. Pustovalova and I. I. Agapov, *Appl. Biochem. Microbiol.*, 2010, **46**, 739.
19. R. L. Horan, K. Antle, A. L. Collette, Y. Z. Wang, J. Huang, J. E. Moreau, V. Volloch, D. L. Kaplan and G. H. Altman, *Biomaterials*, 2005, **26**, 3385.
20. L. Meinel, S. Hofmann, V. Karageorgiou, C. Kirker-Head, J. McCool, G. Gronowicz, L. Zichner, R. Langer, G. Vunjak-Novakovic and D. L. Kaplan, *Biomaterials*, 2005, **26**, 147.
21. X. Q. Wang, T. Yucel, Q. Lu, X. Hu and D. L. Kaplan, *Biomaterials*, 2010, **31**, 1025.
22. J. Kundu, Y. Chung, Y. H. Kim, G. Tae and S. C. Kundu, *Int. J. Pharm.*, 2010, **388**, 242.
23. Z. Zhao, A. Z. Chen, Y. Li, J. Y. Hu, X. Liu, J. S. Li, Y. Zhang, G. Li and Z. J. Zheng, *J. Nanopart. Res.,* 2012, **14**, 736.
24. Z. B. Cao, X. Chen, J. R. Yao, L. Huang and Z. Z. Shao, *Soft Matter*, 2007, **3**, 910.
25. Z. Z. Shao, Z. B. Cao, X. Chen, P. Zhou, J. R. Yao, *CN Pat.*, 1 560 115, 2004.
26. M. J. Chen, Z. Z. Shao and X. Chen, *J. Biomed. Mater. Res. A*, 2012, **100A**, 203.
27. B. S. Davidson, F. Izzo, J. L. Chase, R. A. DuBrow, Y. Patt, D. C. Hohn and S. A. Curley, *Am. J. Surg.*, 1996, **172**, 244.
28. J. L. Grem, *Invest. New Drug*, 2000, **18**, 299.
29. Y. Tsume, J. M. Hilfinger and G. L. Amidon, *Mol. Pharm.*, 2008, **5**, 717.
30. Y. Tsume, B. S. Vig, J. Sun, C. P. Landowski, J. M. Hilfinger, C. Ramachandran and G. L. Amidon, *Molecules*, 2008, **13**, 1441.
31. Y. Tsume, J. M. Hilfinger and G. L. Amidon, *Pharm. Res.*, 2011, **28**, 2575.
32. G. D. Stefano, C. Busi and L. Fiume, *Digest. Liver. Dis.*, 2002, **34**, 439.
33. P. G. Tardi, R. C. Gallagher, S. Johnstone, N. Harasym, M. Webb, M. B. Bally and L. D. Mayer, *Biochim. Biophys. Acta*, 2007, **1768**, 678.
34. X. Fei, M. H. Jia, X. Du, Y. H. Yang, R. Zhang, Z. Z. Shao, X. Zhao and X. Chen, *Biomacromolecules*, 2013, **14**, 4483.
35. X. D. Cui, J. C. Wen, X. Zhao, X. Chen, Z. Z. Shao and J. J. Jiang, *J. Biomed. Mater. Res. A*, 2013, **101A**, 1511.
36. Y. S. Ni, Y. Jiang, J. C. Wen, Z. Z. Shao, X. Chen, S. Sun, H. Q. Yu and W. Li, *J. Biomed. Mater. Res. A*, 2014, **102A**, 1071.
37. J. H. Chen, Q. Yao, D. Li, B. Zhang, L. W. Li and L. Wang, *Cancer Biol. Ther.,* 2008, **7**, 721.
38. J. Liu, H. L. Wong, J. Moselhy, B. Bowen, X. Y. Wu and M. R. Johnston, *Lung Cancer*, 2006, **51**, 377.
39. K. Hirano and C. A. Hunt, *J. Pharm. Sci.,* 1985, **74**, 915.
40. Y. Nishioka and H. Yoshino, *Adv. Drug Deliver. Rev.*, 2001, **47**, 55.
41. C. Oussoren, J. Zuidema, D. J. A. Crommelin and G. Storm, *Biochim. Biophys. Acta*, 1997, **1328**, 261-272.
42. J. Liu, D. Meisner, E. Kwong, X. Y. Wu and M. R. Johnston, *Biomaterials*, 2007, **28**, 3236-3244.
43. B. Subia and S. C. Kundu, *Nanotechnology*, 2013, **24**, 035103.
44. M. Garcia-Fuentes, D. Torres and M. J. Alonso, *Colloid. Surf. B*, 2002, **27**, 159.
45. G. Fontana, M. Licciardi, S. Mansueto, D. Schillaci and G. Giammona, *Biomaterials*, 2001, **22**, 2857
46. J. Araki, M. Wada and S. Kuga, *Langmuir*, 2001, **17**, 21.
47. T. T. Morgan, T. M. Goff and J. H. Adair, *Nanoscale*, 2011, **3**, 2044.
48. B. B. Mandal and S. C. Kundu, *Nanotechnology*, 2009, **20**, 355101.

